GEOPHYSICAL RESEARCH LETTERS, VOL. 28, NO. 18, PAGES 3565-3568, SEPTEMBER 15, 2001

Plasma Transport at the Magnetospheric Boundary due to Reconnection in Kelvin-Helmholtz Vortices

K. Nykyri, A. Otto

Geophysical Institute, University of Alaska, Fairbanks AK 99775-7320.

Abstract. The Kelvin-Helmholtz (KH) mode has long been considered for viscous interaction at the magnetospheric boundary but it is not expected to produce significant mass transport. The presented results indicate that the Kelvin-Helmholtz instability can indeed cause a transfer of mass into the magnetotail during times of northward IMF. The vortex motion of KH waves can generate a strongly twisted magnetic field with multiple current layers. Magnetic reconnection in the strong current layers inside the vortices can detach high density plasma filaments from the magnetosheath. This may explain observed high density and low temperature filaments in the magnetosphere and the correlation of the plasma sheet density and the solar wind density. We present a two-dimensional study of reconnection and mass transport in KH vortices depending on magnetosheath and magnetospheric plasma and field properties. For individual waves the average mass entry velocities is determined to be several km/s.

1. Introduction

The momentum transport by Kelvin-Helmholtz waves into the magnetosphere has long been suggested as a mechanism for the formation of the low latitude boundary layer (LLBL). *Miura* [1984] estimated the momentum transport to be consistent with the transport required to form the LLBL. However, the KH mode is an ideal plasma instability and has therefore not been expected to produce a significant mass transport. Hybrid and full particle simulations indicate that fast anomalous diffusion is possible for sufficiently thin boundaries in the KH vortex [*Fujimoto and Terasawa*, 1994, 1995; *Thomas and Winske*, 1993].

Recent studies [*Keller and Lysak*, 1999; *Otto and Fairfield*, 2000] of the evolution and signatures of KH waves show that KH instability can cause mass transport during periods of strongly northward IMF. The study by *Otto et al.* [2000] has been motivated by Geotail observations in the LLBL at the duskside flank [*Fairfield et al.*, 2000] which showed very large and rapid magnetic field changes in which the B_z component could assume negative values despite the fact that the field on both sides of the LLBL (magnetosheath and plasma sheet) is strongly northward. The simulations demonstrated many detailed properties of the quasi-periodic signatures observed by the Geotail spacecraft by assuming a small magnetic field component along the k vector of the KH mode. Surprisingly the high resolution two-dimensional simulations also demonstrated that magnetic reconnection occurs in the twisted magnetic field of the KH vortices. However, other than a rough estimate of the expected plasma transport, *Otto et al.* [2000] did not study the transport in detail.

This work presents a detailed parameter study to quantify the plasma transport in two dimensions. The reconnection process in KH filaments is sketched in Figure 1. The twisting of the magnetic field leads to anti-parallel magnetic field components generating strong and thin current layers. Finally high density magnetic islands (flux ropes) are detached from the magnetosheath by magnetic reconnection.

This process is not related to so-called vortex induced reconnection which addresses the coupling of KH and tearing mode. Here the magnetic field can be parallel on the two side of the boundary and anti-parallel magnetic field is generated through the KH vortex motion.

2. Numerical Method

The mass transport calculations in this study are obtained with two-dimensional MHD simulations [*Otto*, 1990] in the x,y-plane (approximately the equatorial plane for strongly northward IMF). The initial configuration for the simulation in the boundary coordinates uses a magnetic field of $b_{x0}(x) = b_0(x)sin\varphi$, $b_{y0}(x) = 0$, and $b_{z0}(x) = b_0(x)cos\varphi$ such that $90° - \varphi$ is the angle between the unperturbed magnetic field direction and the k vector of the KH mode. The initial density, pressure,velocity, and magnetic field on the magnetospheric and magnetosheath sides are chosen according to Geotail 1995 event [*Otto and Fairfield*, 2000; *Fairfield et al.*, 2000]. The values for φ, and the magnetic field magnitude are listed in Table 1 for different simulation runs. Length is measured in units of $L_0 = 600$ km and the simulation box is 40 units in x, corresponding to a wavelength of about 4 R_E. The simulation employs 403 × 203 gridpoints in the x and y-directions. The time unit for simulation is expressed in Alfvén times $\tau_A = 5.7$ seconds.

The choice of the resistivity does not appear to be important for the results as long as the resistivity is chosen to avoid fast large scale diffusion. The following four resistivity models are used to demonstrate the influence of the resistivity.

$$\eta(j) = \kappa\sqrt{(j^2 - J_c{}^2)}S(j^2 - J_c{}^2) \qquad (model\ 1)$$
$$\eta(j) = \kappa(j - J_c)S(j - J_c) \qquad (model\ 2)$$
$$\eta(j) = \kappa(j^2 - J_c{}^2)S(j^2 - J_c{}^2) \qquad (model\ 3)$$
$$\eta(j) = 0 \qquad (model\ 4)$$

Here $\kappa = 0.005$ and S is a step function equal to unity for arguments greater than 0 and equal to 0 otherwise. All cases in Table 1 use the current dependent model 1 with a critical current density of $J_c = 1.1J_0 = 24$ nA m^{-2} (model 1a). In addition to cases 1-12 we present results with the

Paper number 2001GL013239.
0094-8276/01/2001GL013239$05.00

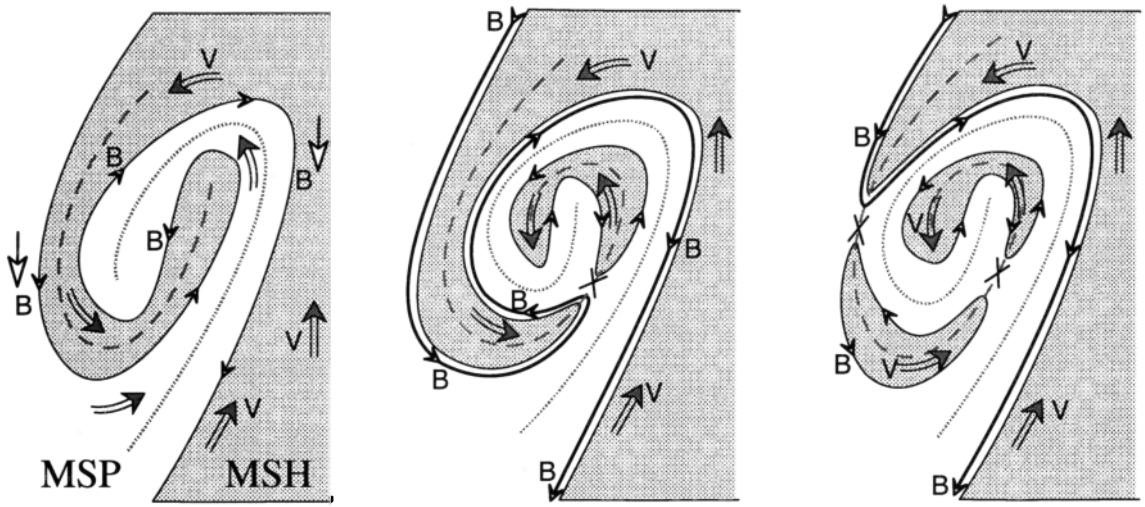

Figure 1. Sketch of the evolution of magnetic reconnection in the Kelvin-Helmholtz vortex

parameters of CASE 5 and the resistivity models 1b, 2, 3, and 4. The model 1b is same as 1a but with the $J_c = 2.1J_0$. Models 2 and 3 use $J_c = 1.1J_0$, and model 4 uses a zero resistivity.

The mass transport is calculated by integrating the plasma density over magnetic islands (flux ropes) captured from the magnetosheath. These islands are defined by plasma elements which are used as tracers for the initial boundary. During the simulation, the location of these elements is determined by integrating the plasma velocity. Ideally the plasma elements stay on the same field line if the magnetic field is frozen into the plasma flow. However, reconnection and numerical dissipation can break this condition.

In two dimensions Ohm's law can be written as

$$\frac{\partial A_z(t)}{\partial t} + (\mathbf{V}\cdot\nabla)\mathbf{A_z(t)} = -\eta \mathbf{J_z}. \qquad (1)$$

A_z is the z-component of the magnetic vectorpotential and changes along the path of a fluid element only due to the resistive term on the right side of (1) if the initial gauge of A_z is maintained. If this is the case a fixed value of A_z determines the magnetic boundary. Since A_z is determined by integrating the magnetic field, we use the plasma elements to determine the proper gauge and to test the frozen-in condition.

Figures 2a to 2c present velocity and density plots for CASE 5, and Figure 2d shows a plot of the time integral $-\int_0^t \eta J_z dt$ versus the value A_z for each plasma element. The scatter is due to numerical dissipation and the gauge is determined by the value of A_z where the regression line of slope 1 crosses the abscissa. The yellow line in the plots of Figure 2 shows the boundary and its deformation as determined by this method.

3. Results

We will describe here the analysis of the CASE 5, with $\varphi = 10°$ for the magnetic field orientation, yielding a positive B_x component of 2.8-4.2 nT on the two sides of the boundary. Figures 2a to 2c illustrate the time evolution of the Kelvin-Helmholtz wave for this case. The plasma density is color coded, lines represent magnetic field lines projected onto simulation plane, and arrows illustrate the orientation and magnitude of the plasma velocity. The asterisks represent plasma elements which were originally at the boundary $y = 0$.

At time $\sim 55.5\ \tau_A$, the KH velocity vortex is twisting the magnetic field, and filamentary current layers are developing fast inside the vortex. No reconnection has occurred up to this time. At time $\sim 74.5\ \tau_A$ (panel B) the KH vortex has further evolved, and a first filament of magnetosheath material (the island in the center of the vortex) is detached from the magnetosheath. Note the periodic boundary conditions at x. The corresponding boundary (yellow line) is determined from Figure 1d. At time $\sim 89.4\ \tau_A$, the main filament is detached similar to the illustration in Figure 1.

The mass entry from the magnetosheath into the magnetosphere is calculated by integrating the density over the area of the detached magnetic islands. An averaged mass entry rate is determined by dividing the mass in the islands through a typical time (i.e. the time it takes to form a nonlinear wave). The results in Figure 3 are expressed in terms of an average entry velocity

$$v_{entry} = \frac{\Delta M}{\Delta t}\frac{1}{\rho_{sh} L_x} \qquad (2)$$

where M is the mass of the magnetic island, Δt is the sim-

Table 1. Simulation Runs

	φ	B in MSP	B in MSH
CASE 1	3°	16 nT	24 nT
CASE 2	3°	24 nT	16 nT
CASE 3	5°	16 nT	24 nT
CASE 4	5°	24 nT	16 nT
CASE 5	10°	16 nT	24 nT
CASE 6	10°	24 nT	16 nT
CASE 7	15°	16 nT	24 nT
CASE 8	15°	24 nT	16 nT
CASE 9	25°	16 nT	24 nT
CASE 10	25°	24 nT	16 nT
CASE 11	35°	16 nT	24 nT
CASE 12	35°	24 nT	16 nT

Summary of cases used in this study

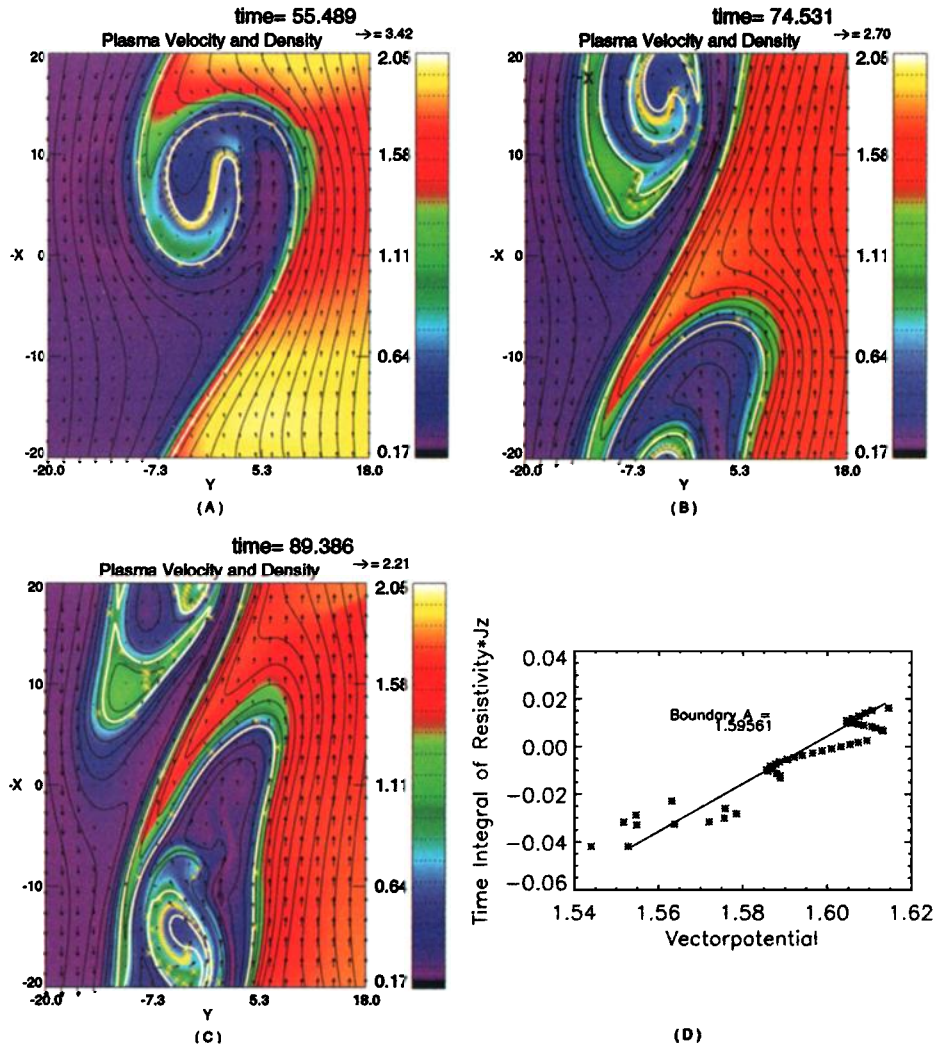

Figure 2. Panel (A) to (C) present the time evolution of Kelvin-Helmholtz wave for CASE 5. The yellow line is the marker for original boundary and yellow asterisks present plasma elements that mark the original boundary $y = 0$. The color measures plasma density, lines are magnetic field lines and arrows are velocity vectors. Panel (D) shows an example of $A_z(t_2)$ versus $-\int \eta J_z dt$ for plot (A) to determine the appropriate boundaries (yellow line in the color plots).

ulation time, L_x is the wavelength and ρ_{sh} is the magnetosheath density.

Figure 3 shows that mass entry starts at time $\sim$ 74.5, and the maximum rate is obtained at time $\sim$ 89.4 corresponding to the detached islands in Figure 2. Errors in the average velocity can be caused by the choice of Δt and inaccuracies of the island boundaries. The time Δt depends on the magnitude of the initial perturbation. In the simulation reconnection starts after about 8 growth times. A reduction of the initial perturbation by a factor of 10 would only change the derived entry velocity by $\sim$ 25 % because of the exponential growth of the mode.

Figure 4 shows the maximum mass entry rates of the 12 simulations and four additional cases with modified resistivity models 1b, 2, 3 and 4. The vertical bars present the error associated with the choice of the island boundary (numerical dissipation). In all cases the mass transport occurs from the magnetosheath into the magnetosphere. The mass entry velocities are of order several km s^{-1}. Assuming a magnetosheath density of 20 particles cm^{-3} and an entry velocity of 1.5 km s^{-1} it would take about an hour to replace the plasma in the plasma sheet with this process (for a plasma sheet density of 1 cm^{-3}) which is in good agreement with corresponding observations [*Borovsky et al.*, 1998]. The mass transport is lower for increasing angle φ,

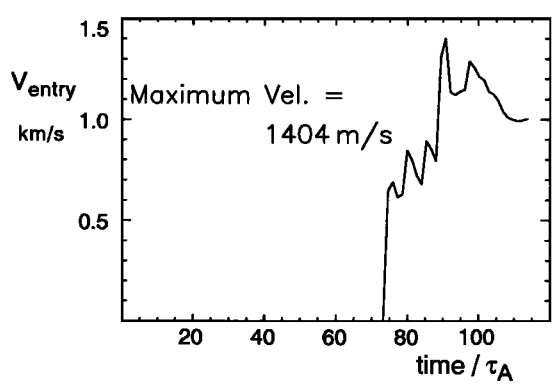

Figure 3. Mass entry velocity as a function of time for CASE 5 ($\varphi = 10$ ° and magnetosheath field strength 24 nT).

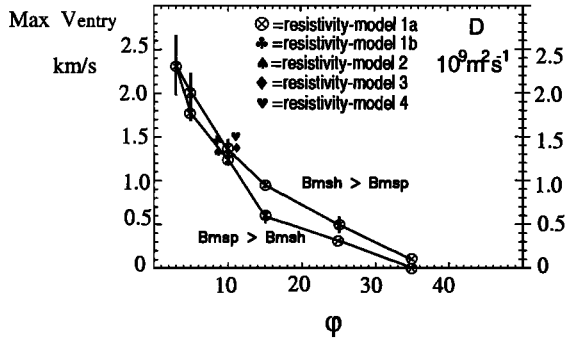

Figure 4. Maximum mass entry velocities with error bars as a function of φ for the cases of Table 1. The scale on the right axis presents the equivalent diffusion coefficient assuming a boundary layer width of 1000 km.

because of increasing stabilization of the KH instability. The scale on the right translates the average entry velocity into a diffusion coefficient for a boundary layer width of 1000 km.

Figure 4 illustrates that magnetic field asymmetry does not have a major effect on average mass entry velocities. For increasing φ a larger asymmetry in the Alfvén speed contributes to the stabilization and may explain the larger relative difference for $\varphi > 15°$. In all cases reconnection always occurs first in the high density filament. We believe that this is caused by the higher inertial forces compared to magnetic forces in these regions of magnetosheath origin. The cases with the modified resistivity (including a 0 resistivity) yield the same mass entry rates within the error margin of the other cases. They demonstrate that the resistivity does not appear to alter the results significantly, and that the dynamics is strongly governed and driven by the ideal KH vortex evolution.

The average entry velocity should not depend much on the wavelength of the mode as long as inhomogeneities do not alter the growth significantly. In equation (2) the numerator scales with the square of the wavelength and the growth time is proportional to the wavelength such v_{entry} is to lowest order independent of the wavelength.

4. Summary and Discussion

Our 2-D MHD simulations indicate that during periods of northward IMF, magnetic reconnection inside Kelvin-Helmholtz vortices can provide a major mass transport mechanism from the solar wind into the magnetosphere. For single wave modes we obtain mass entry velocities of several km/s. This is in excellent agreement with observations [*Fujimoto et al.*, 1998] which show the presence of high density and low temperature plasma blobs in plasma sheet, turbulent flow in a plasma sheet and a 2-hour correlation in the plasma sheet density in response to changes in solar wind plasma [*Borovsky et al.*, 1998].

The mass entry is reduced for an increasing magnetic field in KH plane, because a larger parallel field stabilizes the KH wave. Our results indicate that considerable mass transport can be expected for magnetic field rotations of less than $\sim 50°$. An asymmetry of the magnetic field strength across the magnetopause does not have a significant influence on the plasma transport.

The presented two-dimensional results are a necessary first step to understand the plasma transport associated with KH modes. In two dimensions we have assumed that the magnetospheric boundary is represented by the initial shear flow boundary. A 2-D model does not provide any information on how magnetic field is connected in the third dimension which requires three-dimensional studies. In three dimensions we expect the process to produce a more complex magnetic connection with a portion of the LLBL on open field lines and a portion on closed field lines. While the precise quantitative transport may change in three dimensions, the basic mechanism and its properties will be present in three dimensions.

Another limitation of the present results is the assumption of MHD dynamics. In particular thin current sheets may require to include physics on the ion inertia scale. However, the presented results demonstrate that reconnection is strongly driven by the twisting of the magnetic field in the vortex motion. Changes caused by the resistivity are minor as long as the magnetic diffusion remains sufficiently small to permit the formation of the filamentary currents. Thus the net plasma transport might not be very sensitive to the details of the plasma approximation.

Acknowledgments. The research was supported by the NASA SR&T Grant NAG-9457. In addition Katariina Nykyri's work is supported by Finnish Cultural Foundation, Finnish Academy and Jenny and Antti Wihuri Foundation of Finland. The computations were supported at the Arctic Region Supercomputer Center.

References

Borovsky, J. E., M. F. Thomsen, and R. C. Elphic, The driving of the plasma sheet by the solar wind, *J. Geophys. Res.*, *103*, 17,617, 1998.

Fairfield, D. H., R. P. Lepping, A. Otto, T. Mukai, T. Yamamoto, S. Kokubun, J. T. Steinberg, and A. J. Lazarus, Geotail observations of the Kelvin-Helmholtz instability at the eqatorial magnetotail boundary for parallel northward fields, *J. Geophys. Res.*,*105*, 21,159, 2000.

Fujimoto, M., and T. Terasawa, Anomalous ion mixing within an MHD scale Kelvin-Helmholtz vortex, *J. Geophys. Res.*, *99*, 8601, 1994.

Fujimoto, M., and T. Terasawa, Anomalous ion mixing within an MHD scale Kelvin-Helmholtz vortex, 2, Effects of inhomogeneity, *J. Geophys. Res.*, *100*, 12,025, 1995.

Fujimoto, M., T. Terasawa, T. Mukai, Y. Saito, T. Yamamoto, and S. Kokubun, Plasma entry from the flanks of the near-Earth magnetotail: Geotail observations, *J. Geophys. Res.*, *103*, 4391, 1998.

Keller, K. A., and R. L. Lysak, A two-dimensional simulation of kelvin-helmholtz instability with magnetic shear, *J. Geophys. Res.*, *104*, 25,097, 1999.

Miura, A., Anomalous transport by magnetohydrodynamic Kelvin-Helmholtz instabilities in the solar wind magnetosphere interaction, *J. Geophys. Res.*, *89*, 801, 1984.

Otto, A., 3D resistive MHD computations of magnetospheric physics, *Comput. Phys. Commun.*, *59*, 185, 1990.

Otto, A., and D. H. Fairfield, Kelvin-helmholtz instability at the magnetotail boundary: Mhd simulation and comparison with geotail observations, *J. Geophys. Res.*, *105*, 21,175, 2000.

Thomas, V. A., and D. Winske, Kinetic simulations of the Kelvin-Helmholtz instability at the magnetopause, *J. Geophys. Res.*, *98*, 11,425, 1993.

K.Nykyri, A. Otto, Geophysical Institute, University of Alaska, Fairbanks, AK 99775-7320. (e-mail: ftkk@aurora.alaska.edu; ao@how.gi.alaska.edu)

(Received March 28, 2001; revised May 29, 2001;
accepted June 18, 2001.)